RADIO SPIKES AND THE FRAGMENTATION OF FLARE ENERGY RELEASE

A. O. BENZ

Institute of Astronomy, ETH, Zürich, Switzerland

(Received 11 January, 1985)

Abstract. Decimetric radio events with large numbers of spikes during the impulsive phase of flares have been selected. In the observing range of 100 to 1000 MHz some flares have of the order of 10000 spikes or more. The average half-power bandwidth of spikes has been measured to be only 1.5% of the spike frequency. Since the emission frequency is determined by some source parameter (such as plasma frequency or gyrofrequency) the source dimension must be a small fraction of the scale length. From the flare configuration a typical upper limit of the dimension of 200 km is found. The observed fragmentation in the radio emission cannot be explained by a patchy emission mechanism of a single and much larger source without an additional (and unknown) assumption. It is proposed that the fragmentation already occurs in the exciter.

Four events were analyzed in detail and compared to UV, SXR, and HXR data. The density of the loops where the SXR and HXR emission was observed has been measured before the flare. The plasma frequency well agrees with the observed frequency of spikes. The spikes thus originate close to or in the energy release region. It is suggested here that the fragmentation of the exciter is due to a fragmentation of the primary energy release. Each of these 10^4 'microflares' would release an energy of the order of 10^{26} erg within 0.05 s.

1. Introduction

Radio emission spikes of less than 0.1 s duration have attracted increasing interest in recent years. They have first been reported by Dröge and Riemann (1961), de Groot (1962), and Elgarøy (1962) at frequencies between 210 and 330 MHz. Since then, spikes have been observed by more than a dozen of instruments from 20 MHz (Barrow and Saunders, 1972) up to 2840 MHz (Zhao and Yin, 1982). They generally occur in groups and their total activity lasts of the order of 100 s or less. Their bandwidth is typically $\leq 2\%$ of the center frequency (with an exceptional large bandwidth type noted by Tarnstrom and Philip (1972a) which we do not consider here). Several attempts to identify the emission process have been made. Early ideas include electron cyclotron emission (Malville *et al.*, 1967) and plasma emission (Tarnstrom and Philip, 1972b). The cyclotron mechanism has been quantitatively investigated and applied to spikes by Melrose and Dulk (1982) and Sharma *et al.* (1982). Detailed calculations on the plasma emission process have been carried out for Langmuir waves by Zheleznyakov and Zaitsev (1975) and Kuijpers *et al.* (1981) and for upper-hybrid waves by Vlahos *et al.* (1983). Recently, Benz *et al.* (1982) have suggested a variant to the plasma hypothesis in which the duration and bandwidth (i.e. source size) of a spike is not determined by the bump-in-tail instability but by the spatial extent of a high level of low-frequency turbulence typical for current instabilities (in analogy to a model for type I radio bursts by Benz and Wentzel, 1981).

Solar Physics **96** (1985) 357–370. 0038–0938/85.15

Are all spikes the same? Spikes have been observed during type I, III, IV, and microwave bursts. Even if the mechanism were the same, the source environments are probably not. This is particularly obvious for the ratio of plasma frequency to gyrofrequency, a parameter which is crucial for cyclotron (maser) emission. Conditions also vary at different frequencies for free-free absorption, which is critical for fundamental plasma emission. Already Elgarøy (1962) and Malville *et al.* (1967) have noted that there seems to be a continuous transition from type I bursts to associated spikes. Benz *et al.* (1981), however, find type III associated spikes to differ from type I bursts in their distribution over the disk, in polarization, and in clustering. For the type III associated spikes these authors observe predominantly low and intermediate polarization. This is contrary to spikes during type I storms as well as to spikes associated with decimetric type IV bursts (deGroot, 1962), and at 2.6 GHz, where strong polarization up to 100% has been reported (Slottje, 1980).

The question on the number of spike producing processes cannot be decided here. This investigation is limited to spikes in the decimetric band (300–1000 MHz). Fine structure spikes in type IV bursts ('rain') and in noise storms (type I) are excluded. Wiehl *et al.* (1984) find that the remaining spikes are generally associated with metric type III bursts. Starting from type III bursts, Benz *et al.* (1981) reported that at least 10% (but possibly more than 20%) of the type III bursts show spikes near their beginning (in time and frequency). Large groups of spikes, generally classified as DCIM ('decimetric pulsations') have been compared to hard X-rays (HXR) by Kane and Benz (1985). They have found enhanced HXR emission in 71% of all cases. This is a very high association rate compared with 3% for metric type III bursts (Kane, 1981) and with 45% for decimetric type III bursts (Aschwanden *et al.*, 1985). The occurrence of radio spikes generally starts after the HXR emission and has a shorter duration. Maximum spike activity has a tendency (1.4 standard deviations) to occur before maximum HXR flux (Kane and Benz, 1985). Although this is not statistically significant, it is contrary to all other types of decimetric bursts (except type III-like events). This difference is statistically significant.

Elementary flares have been proposed by de Jager and de Jonge (1978) to interpret HXR peaks of average half-power durations of 4–24 s. This is also a typical time between type III bursts. In fact, in several cases a correlation between HXR peaks and type III bursts has been reported (Kane *et al.*, 1982; Dennis *et al.*, 1984).

Here I present evidence that radio spikes associated with type III bursts indicate even smaller fractions of flare energy release. More than 10 spikes per type III event were observed in the events studied by Benz *et al.* (1982). For the 'richer' groups studied here this number often exceeds 100 per type III burst, bringing the total number per flare to several thousand. The first calibrated spectra of spikes are presented. The bandwidth of individual spikes has been accurately measured. The spike data has been combined with HXR and other observations to locate the radio source. Its density is identical with the preflare density of the flare region as determined from UV and SXR measurements. It is suggested here that each spike is a microflare, in which energy first is released into a tiny volume.

2. Observations

2.1. Instruments and selection

The radio observations have been made with the frequency-agile ETH spectrometer (IKARUS) in Bleien (Perrenoud, 1982). An on-line minicomputer detects the burst activity and records the full information and calibration data on tape. The system was operating with a time resolution of 0.1 s, at 200 frequency channels, and with a channel bandwidth of 3 MHz. The channels were arranged into 8 bands spread between 100 and 1000 MHz. These observations are complemented by an older, film-recording analog spectrograph (DAEDALUS). We have identified 37 large spike events among 664 decimetric bursts classified as DCIM in 1980 and 1981 (Wiehl *et al.*, 1984). The fraction of bursts with some spikes is expected to be larger, since the procedure was not suitable for detecting spikes except in large numbers. This set of large spike events is used here for statistics on global parameters. Most of these events have a much larger number of spikes (one or two orders of magnitude) than the spike clusters investigated by Benz *et al.* (1981). The present spikes mostly occur at frequencies above the starting frequency of the associated type III bursts. They are in all their properties compatible with the most frequent class of spikes (*B*) defined by Benz *et al.* (1981).

Four homologous events have been further selected for detailed analysis. They occurred on 1980, August 31 in two pairs, the first pair starting at 09 : 23 UT and the second at 12 : 48 UT. The events in each pair were separated by only a few minutes. They were associated with simple compact flares of modest intensity ($\leq$M2 in GOES classification), and all of them occurred in the same part of the active region Hale Nr. 17098. The radio observations of the second pair are presented in Figure 1 as an example. The metric type III bursts and the spikes can be easily separated even on film records for the 12 : 52 UT flare due to their different intensity. The emissions of type III and spikes do not overlap in frequency. They are clearly separated between 370 and 400 MHz. The separation line reaches a maximum in frequency at maximum HXR flux. The 12 : 49 UT event in fact is very similar, but more intense and has in addition some decimetric type U bursts at 12 : 49 : 10 UT, discussed by Strong *et al.* (1984) and a broadband, fluctuating continuum (patches) at frequencies above 830 MHz at 12 : 49 UT.

Both type III and spike bursts are coincident with enhanced HXR emission in agreement with the statistics of Aschwanden *et al.* (1984). Strong *et al.* (1984) have estimated the partition in thermal, non-thermal, and kinetic energy in these flares from X-ray emissions. In the impulsive phase of the flares of Figure 1 the HXR emitting electrons represent 40%, resp. 30% of the total flare energy. The spikes thus occur in the primary phase of energy release in the flare. Whereas in the 12 : 49 UT event the spikes start simultaneously with HXR, in the 12 : 52 UT flare they abruptly set in about 40 s after the start of HXR, at the time of the sharp increase in HXR flux. As Strong *et al.* (1984) point out, soft and hard X-ray data indicate that the first flare of the pair considerably changes the plasma conditions of the second flare (higher density and temperature). It seems that this change also reduces the visibility of the spikes. Despite

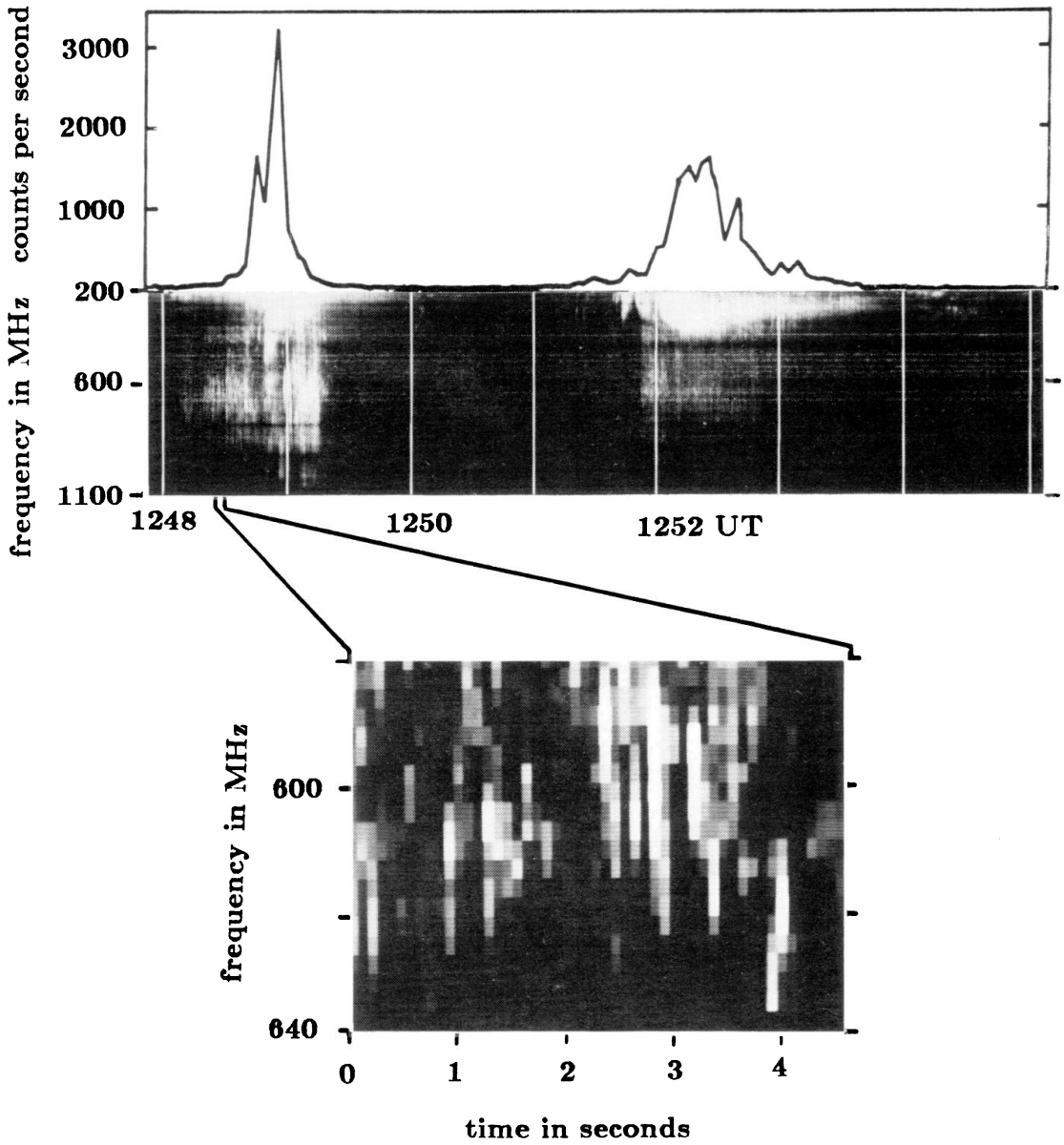

Fig. 1. A pair of flares with decimetric spikes on 1980, August 31. *Top*: Composed figure showing HXR counts vs time (≥ 30 keV, observed by HXRBS on board SMM, courtesy Dr. B. R. Dennis), and radio spectrogram registered by the analog spectrograph (Daedalus). The spectrogram shows type III bursts at metric wavelengths and spike activity above about 350 MHz. *Bottom*: Blow-up of a small fraction of the spectrogram produced from data of the digital spectrometer (Ikarus) presenting single spikes.

the higher energy of the second flare (1.5×10^{30} vs 1.0×10^{30} erg) the spikes are weaker and less numerous. Since other basic spike properties, such as center frequency and bandwidth remain unchanged, the erratic appearance may be interpreted as an absorption or propagation effect.

2.2. Bandwidth of spikes

The spikes in Figure 1b have a duration of less than 100 ms, the instrumental resolution. This is compatible with the half-power durations of 20–50 ms measured by Benz *et al.*

(1981) at 315 MHz. However, the spectra of some random single spikes presented in Figure 2 demonstrate that he spikes have been resolved in frequency. Their spectral half-power width is typically 10 MHz or 1.5% of the center frequency. The strongest spike in the 1249 UT flare reaches a flux of 1600 sfu (1.6×10^{-16} erg cm^{-2} Hz^{-1} s^{-1}).

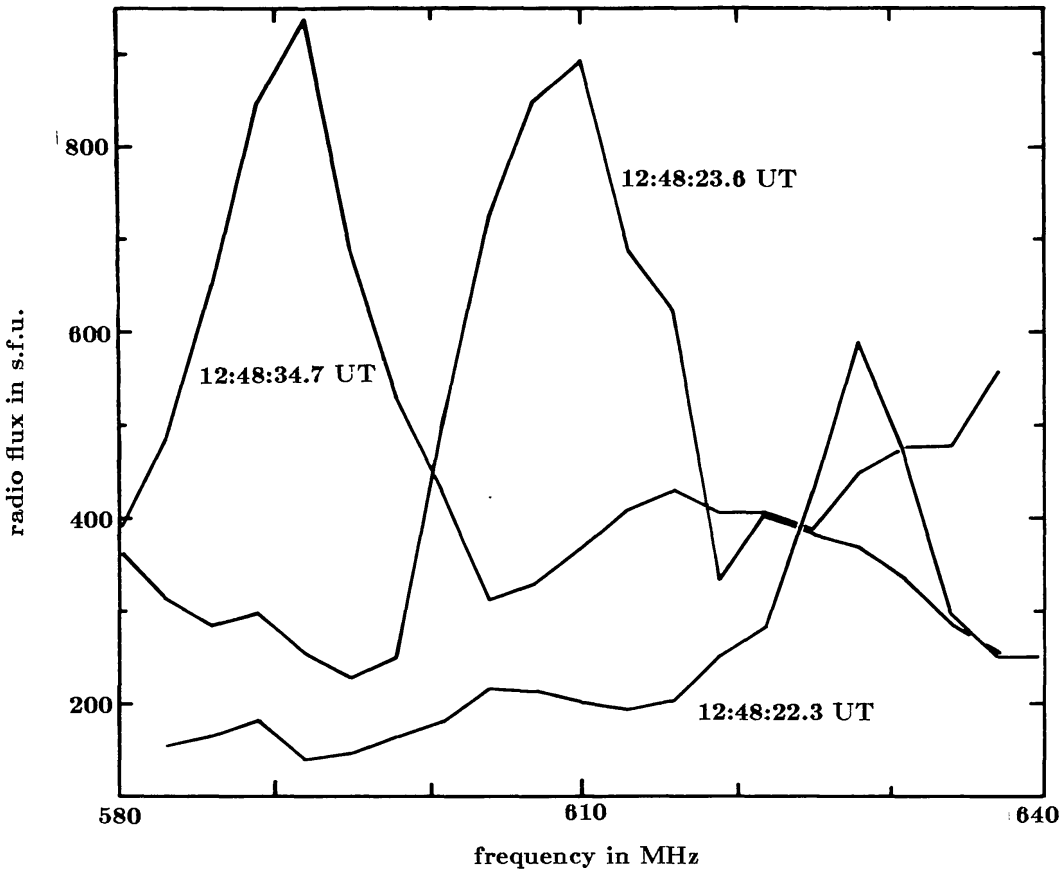

Fig. 2. Calibrated spectra of three isolated spikes of the 12 : 49 UT flare. Each spectrum in the figure was taken by a single sweep in frequency within 10 ms.

The total bandwidth (above noise) has been measured in the first 100 isolated spikes in each frequency band. Figure 3 shows that the total bandwidth $\Delta\nu$ increases with frequency ν. The average is roughly 2% of the center frequency in the band from 350 to 1000 MHz. There is a tendency for a deviation from linearity to smaller bandwidths at 1000 MHz.

2.3. Number of Spikes

Spikes exceeding 5 standard deviations can easily be counted in digital data. The total number can only be estimated since the data is undersampled in time and has gaps in frequency. The frequency-agile receiver measures only 0.5 ms at a given frequency and comes back to the same frequency 100 ms later. From observations at higher resolution (Benz *et al.*, 1982) it is estimated that about half of the spikes have been missed in the present data. The frequency gaps can be interpolated from spectral representations such

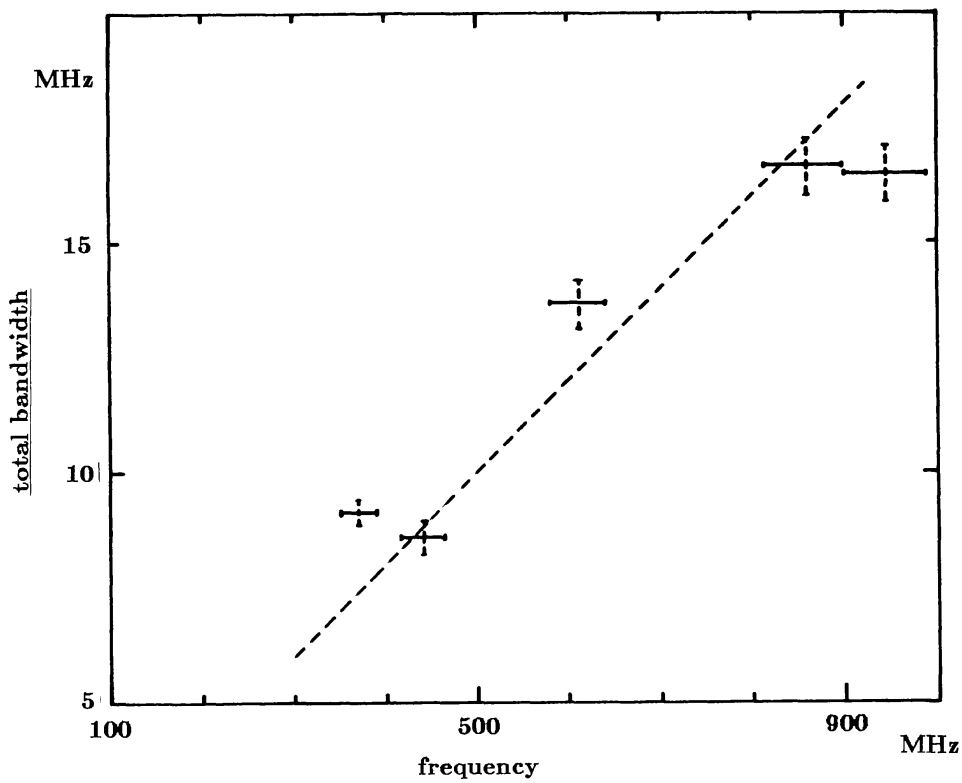

Fig. 3. Total bandwidth of spikes vs. center frequency of the 12 : 49 UT flare. The dashed line represents the line of 2% bandwidth ($\Delta\nu = 0.02\,\nu$).

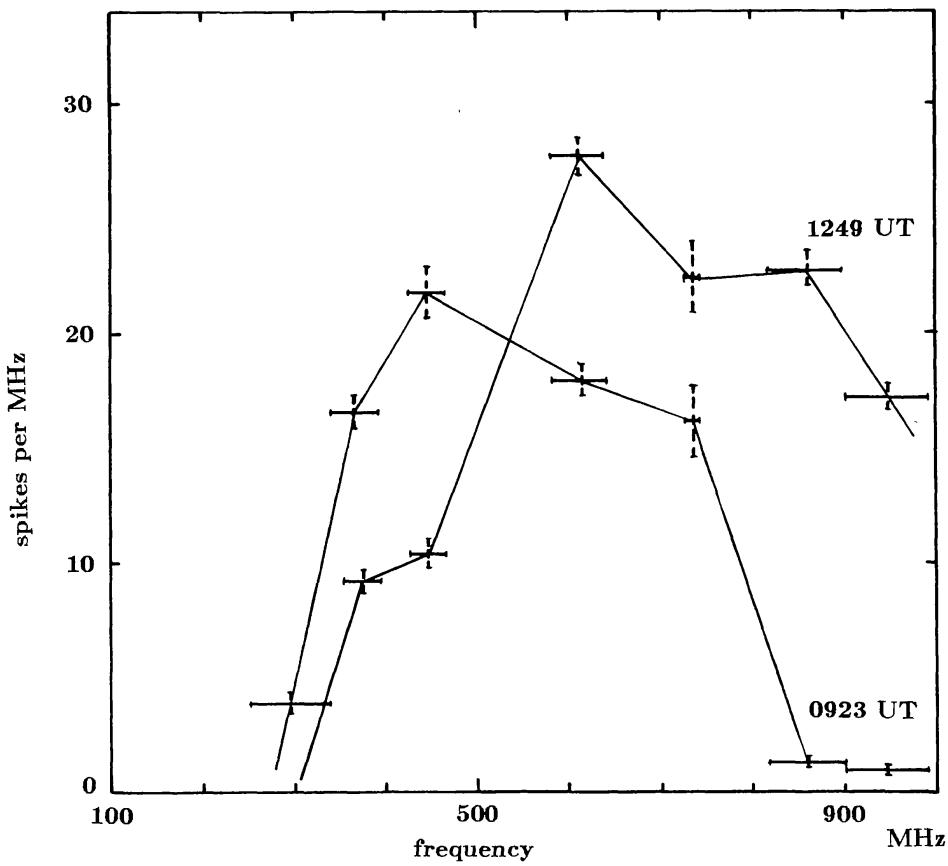

Fig. 4. Number of spikes per MHz in the various frequency bands for two flares. A correction factor of 2 has been used to account for undersampling.

as Figure 4, where the spike rate per unit frequency was determined from counts in each frequency band divided by the width of the frequency band. The number was doubled to correct for undersampling in time. The spikes of the 09 : 23 UT flare seem to be within the observing range of frequency. The total number of spikes in this flare is estimated to be 8200. The spikes of the 12 : 49 UT flare extend beyond the highest observing frequency. The number of spikes below 992 MHz, about 13 200, is only a lower limit.

Figure 5 compares te number of spikes per second with the integrated radio flux of the spike emission. The spike rate reaches a nearly constant level of about 230 s^{-1} very early in the flare. The spike flux, however, increases until about the time of peak HXR flux. The radio emission between 12 : 48 : 50 and 12 : 49 : 17 UT is dominated by broadband patches. The patches seem to reduce the visibility of the spikes causing dips in the spike rate around 12 : 49 UT.

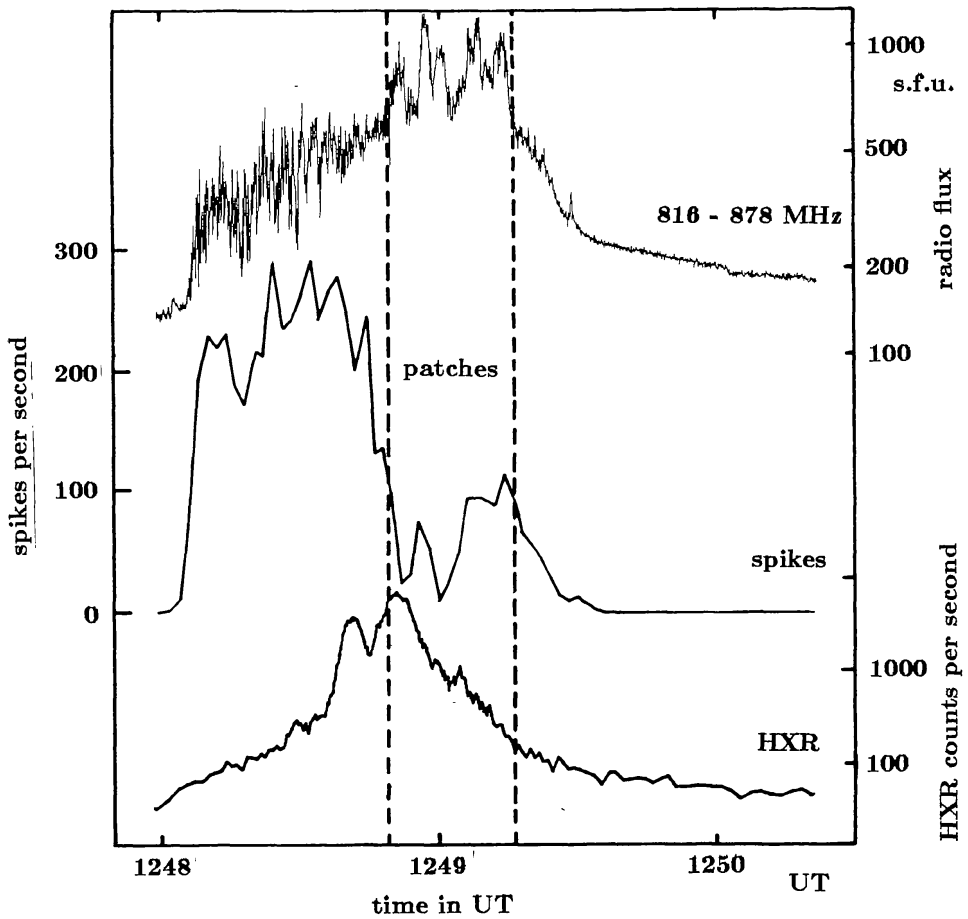

Fig. 5. Comparison of spike rate (*middle*) with average spike flux in a large frequency band (*top*) and HXR flux at energies ≥ 30 keV (*bottom*, courtesy B. R. Dennis, HXRBS/SMM). The spike rate has been corrected for undersampling and frequency gaps, but is limited to frequencies below 1000 MHz.

2.4. Polarization of Spikes

The circular polarization of representative spikes in each frequency band has been measured. Their polarization was found to be intermediate and to have a large scatter.

There are also systematic trends. In the 12:49 UT flare e.g. the average spike polarization in the 580–646 MHz band changed from 28% R early in the flare to 56% R later. This temporal variation is more significant than the variation in frequency. In Figure 6 the distribution of polarization measurements of spikes is shown. They have been selected from the same time interval but in all frequency bands.

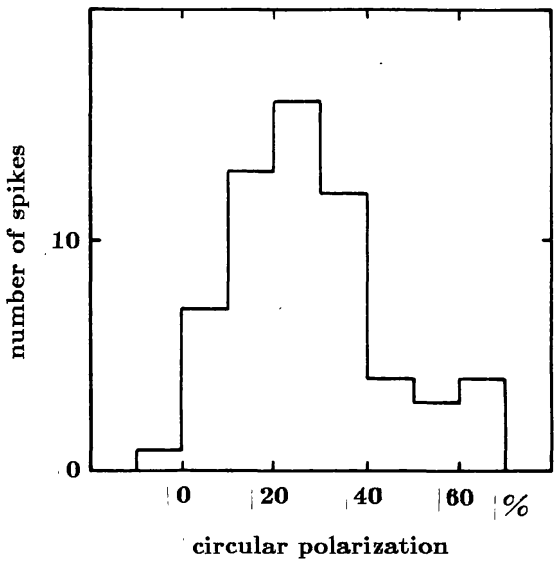

Fig. 6. Distribution of circular polarization of spikes (positive = right polarized). The figure summarizes the measurements of 60 spikes in the early phase of the 12:49 UT flare distributed over the whole range of frequencies where spikes have been observed.

2.5. Correlations

Figure 7 presents the correlation of average spike flux with metric type III emission and HXR. The selected frequency band for the spikes is free of other emissions for the two flares except for one decimetric type III burst at 09:24:20 UT. The correlation with metric type III bursts is remarkable, although there is not a peak-to-peak correlation (cf. Figure 7b). The metric emission has a prolonged decay which is partially caused by a type V-like continuum. The most noticeable deviation is at 09:26:30 UT when two large type III bursts occurred before the peak in spike activity about 7 s later. In this case the HXR follows the trace of the type III flux. Such a delay of the spikes in relation to the type III has not been observed by Benz *et al.* (1982) and seems to be exceptional. The type III emissions at lower frequency (higher altitude), in the 100–145 MHz and 160–175 MHz bands, have also been compared. They correlate less, which is to be expected from the larger separation of the radio and HXR sources. The observed correlations in Figure 1, 5, and 7 clearly demonstrate the close connection of spikes and energetic electrons.

2.6. Flare configuration

Strong *et al.* (1984) have analyzed the conditions in the flare region. They suggest that the interaction of small and large loops released the magnetic energy stored in the stress

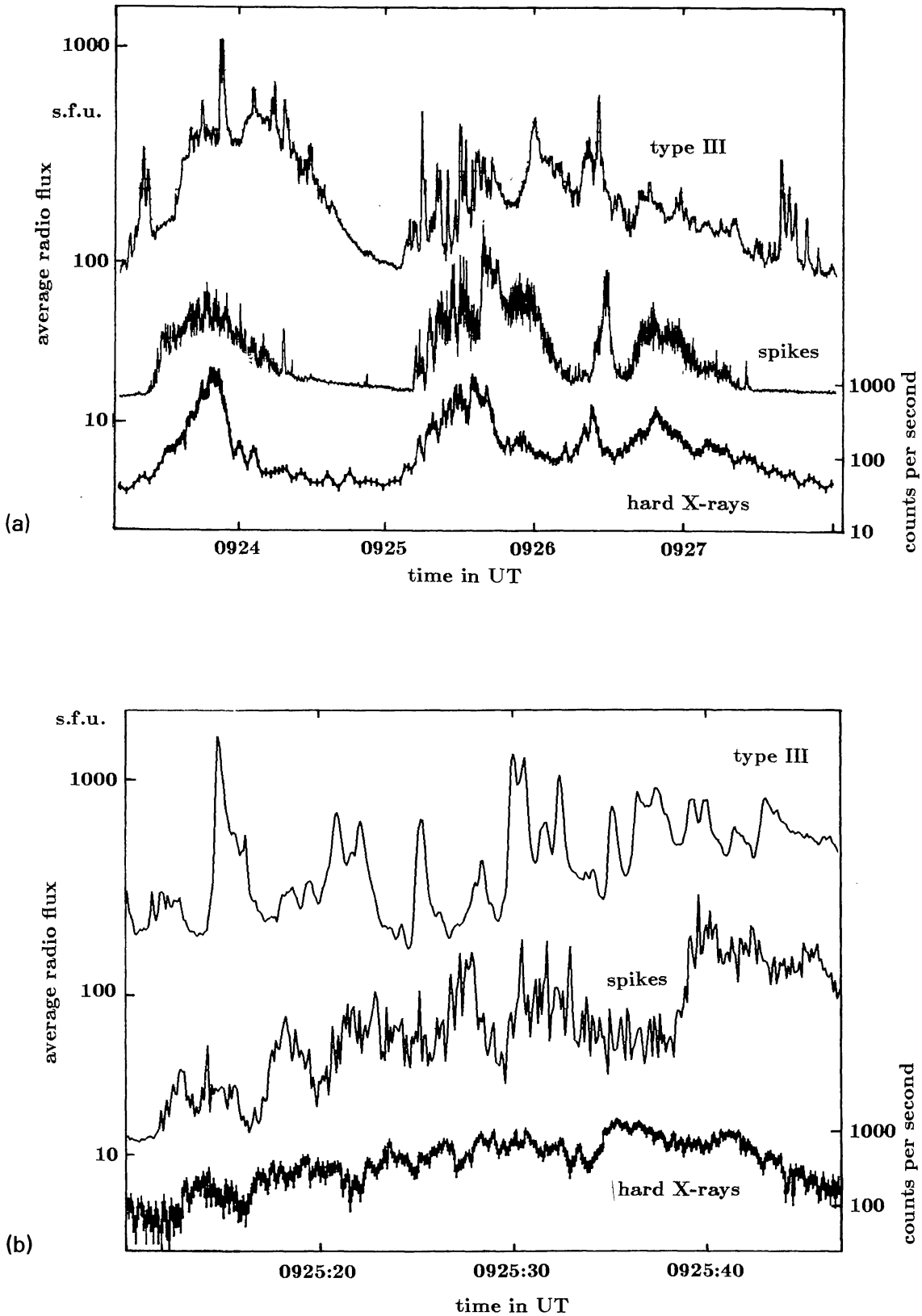

Fig. 7. Correlation of average spike flux in the frequency band 580–640 MHz (*middle*) with type III emission in the 250–310 MHz band (*top*) and HXR (*bottom*), courtesy B. R. Dennis, HXRBS/SMM. (a) The time profiles of the first pair of flares on August 31, 1980. (b) An enlargement of a part of (a). The HXR data is shown with error bars.

of emerging small loops. A possible configuration is shown in Figure 8. The small loops have been seen in projection in SXR and HXR. The large loops are indicated by HXR footpoints and decimetric U-shaped bursts characteristic for electron beams in loops. Strong *et al.* find from the SXR emission a density of the flare region (small loop) before the first flare (12:49 UT) of $3–4 \times 10^9$ cm^{-3} at $2.5–3 \times 10^6$ K. It corresponds to a plasma frequency of 500–600 MHz. This frequency is in the range of observed spikes and starting frequency of U-bursts. The agreement suggests that spikes originate close to or in the flare region.

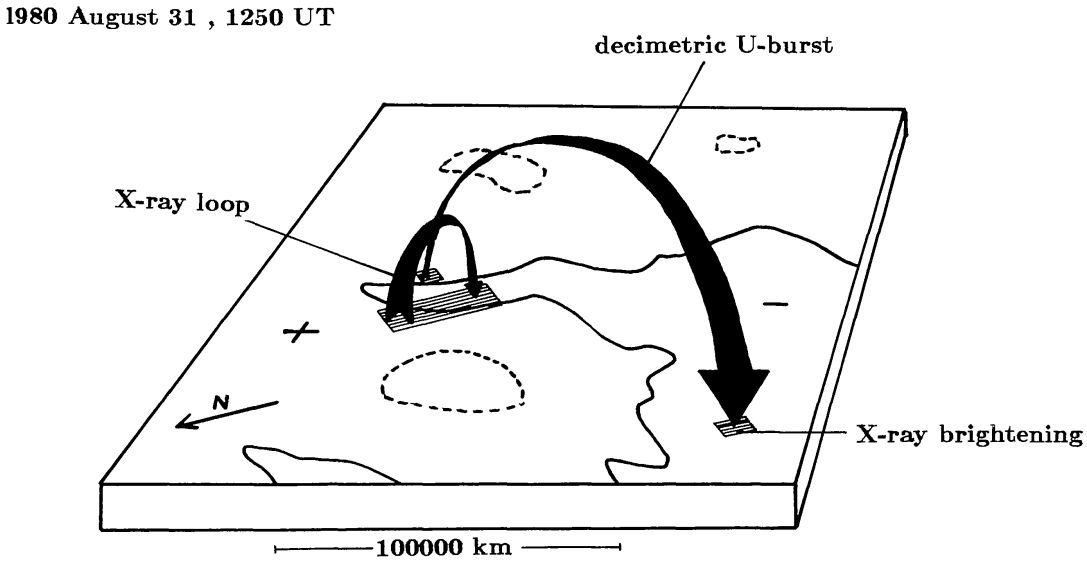

Fig. 8. Sketch of flare region based on the study by Strong *et al.* (1984). The line of neutral longitudinal magnetic field is shown. Sunspots are outlined with dashed curves. Hatched are regions of enhanced HXR emission. Possible large and small loops are indicated.

It is interesting to note that the SXR emission before the second flare yields a density of 3×10^{11} cm^{-3} at 5×10^6 K. The spikes and U-bursts, however, are not observed at the correspondingly 10 times higher plasma frequency, but at about the same frequencies or even lower. SXR emission, being proportional to the square of the density, only measures the high density structures. A likely interpretation is that the spikes and U-bursts occur on field lines which have not been involved in the energy release of the first flare and still have preflare density.

3. Interpretation of Spikes as Microflares

3.1. Source Dimension

Several emission processes for spikes have been proposed (cf. Section 1). The emission frequency of all models is either the local plasma frequency, ω_p, or the electron gyrofrequency, Ω_e. Take for example trapped particles in a magnetic loop having a loss-cone

distribution in velocity space. An electron cyclotron (maser) instability may then occur if the electron cyclotron frequency is comparable or larger than the plasma frequency. In the above scenario the observed frequency ω equals the local gyrofrequency (or one of its harmonic):

$$\omega = \Omega_e = s \frac{eB}{mc} \qquad (s = 1, 2, \ldots) . \tag{1}$$

To allow spikes in the observed range (400–1000 MHz), the magnetic field must change by at least a factor of about e within the volume of the exciter. It is unlikely that this volume corresponds to the large loop in Figure 8, since type U bursts in this structure emit at a lower frequency. Very likely the volume is of the size of the small loops (or smaller) and the magnetic scale length λ about 10 000 km or smaller. The source dimension l of a spike is determined by the bandwidth of the spike:

$$l = \lambda \frac{\Delta\omega}{\omega} \leq 200 \text{ km} . \tag{2}$$

A similar value results if plasma emission is assumed. This is an order of magnitude smaller than the 'speed of light dimension' derived from the duration of spikes (but compatible if the Alfvén speed is used (Slottje, 1978)).

3.2. Secondary Fragmentation

The observed fragmentation of the decimetric radiation into spikes may either be a secondary effect of one (or a few) global energy release process, or it may reflect a fragmentation of the energy release proper. I will first argue that the first possibility requires an ad hoc assumption on the bandwidth of spike emission and/or on the spike duration, and then discuss the second possibility. Secondary fragmentation may occur if the exciter extends over a large source volume, but becomes visible only locally for a short time. The localization of the source of emission may be caused by some inhomogeneity in the background plasma or fields. However, such a spatial interpretation cannot explain the temporal properties, unless the duration of these inhomogeneities is limited to 20–50 ms. This value is of the order of the electron-electron collision time and excludes any simple MHD process. Therefore, some additional mechanism is required to limit the spike emission in both time and frequency.

3.3. Fragmentation by the Flare Energy Release

To economize assumptions I propose here that the fragmentation of the radio emission into spikes is he result of a discontinuous exciter (beam, current, etc.). Since the density measurements indicate that the spike sources are close to or in the energy release region, I suggest that the fragmentation of the exciter is due to discontinuous energy release. From this assumption several important conclusions follow:

(1) The large scatter of spike frequencies suggests that the energy release occurs at many different sites.

(2) At each site the energy is released into a small volume since the resulting spikes have small sources.

(3) The typical energy of such a 'microflare' (the total flare energy divided by the number of spikes) is of the order of 10^{26} erg for the four flares studied in detail.

The 10000 microflares would need a trigger to occur within 50–100 s, such as non-thermal particles or waves. To become visible in radio waves, these microflares must accelerate particles, excite plasma waves or both. Energetic particles may after some propagation become unstable towards growing Langmuir waves or upper-hybrid waves or directly emit radiation by the electron cyclotron (maser) instability.

How is the emission region of such a beam limited to less than 200 km? Here I suggest that the spike source is identical with the site of energy release. Since magnetic energy can only be released by a current, the spike sources are tentatively identified with places of some current instability. Ampère's law limits the size of unstable currents (in one or two dimensions) and yields a natural reason for a small width d in the direction of the field gradient:

$$d \approx \frac{cB}{4\pi j} = \frac{c\Omega_e}{\omega_p^2}\,\frac{c}{v_D}\,, \tag{3}$$

where the plasma frequency, ω_p, is given by the observing frequency (assuming fundamental emission). Assuming a current drift velocity v_D equal to the thermal ion speed (which is typical for current instabilities) and $\omega_p \approx \Omega_e$, $d \approx 0.1$ km. For a current sheet the other two dimensions could be much larger. They may be estimated from the total energy estimated per microflare,

$$E = \frac{d_1 d_2 d_3\, B^2}{8\pi} \approx 10^{27}\ \text{erg} \tag{4}$$

The total width d_1 may be much larger than the instantaneous width derived in Equation (3). An upper limit is the product of duration of a spike times Alfvén velocity leading to $d_1 \leq 350$ km. Equation (4) then yields $d_2 \approx d_3 \leq 880$ km. Unstable current sheets accelerate particles by the run-away process and/or by resonant acceleration of wave turbulence. Unstable currents are known to have low-frequency turbulence. There are several possible emission processes. A detailed analysis is required to identify the most likely mechanism.

4. Conclusions

Radio spikes are commonly seen during the impulsive phase of compact flares, particularly at decimetric wavelengths. Their bandwidth on the average is 1.5% of the center frequency measured at half-power of the peak. Since the emission must be at a characteristic frequency of the source (plasma frequency or gyrofrequency), the relevant source parameter cannot vary more than this amount. The appropriate scale length then limits the source site (typically to 200 km). The bandwidth of a single spike is a small

fraction (2%) of the total band over which spikes are scattered. In four cases analyzed in detail the observed frequency of spikes corresponds about to the plasma frequency at the flare site before the event.

The simplest interpretation of the observed myriads of spikes is that the energy of a flare is released in thousands of 'microflares'. They have tentatively been identified with sites of current instability in the reconnection flare model. Each microflare would release of the order of 10^{26} erg in the form of heat, low-frequency waves, and accelerated particles. Only 10^7 erg are emitted as a radio spike. Detailed models only can decide on the predominant emission mechanism. Two constraints have become clear in this study:

(1) The energy consideration (Equation (4)) suggests $\Omega_e \geq \omega_p$. If the magnetic field were assumed much smaller, the dimensions d_2 and d_3 would exceed the speed of light dimension (6000 km). The emission mechanism may thus be different from the $\Omega_e < \omega_p$ plasma of the type I burst sources believed to be Langmuir wave emission.

(2) The emission is limited to a very small source. Its dimension is comparable with the expected region of energy release. The simplest assumption is to put these two regions identical and to assume that the bandwidth of a spike is given by the size of the region of energy release.

The source regions of type III bursts and HXR peaks ('elementary flare events') may be thousands of kilometers away from the acceleration sites and in this interpretation seem to be the integrated effects of many (order of 100) acceleration events in microflares. A remarkable global correlation of type III emission and HXR with spikes is found. The details of these emissions, however, do not always coincide.

Spike emission may be an instantaneous radiation of a microflare. This would explain the tendency of spike activity to occur before some other types of decimetric emission.

Acknowledgements

Hard X-ray data has kindly been provided by B. R. Dennis from the HXRBS team of the Solar Maximum Mission. I also acknowledge helpful discussions with K. Appert and J. Vaclavik at Centre de la Physique des Plasmas in Lausanne. The construction of the Zürich spectrometers is being financially supported by the Swiss National Foundation (grant No. 2.460–0.82).

References

Aschwanden, M. J., Wiehl, H. J., Benz, A. O., and Kane, S. R.: 1985, *Solar Phys.*, in press.
Barrow, C. H. and Saunder, H.: 1972, *Astrophys. Letters* **12**, 211.
Benz, A. O. and Wentzel, D. G.: 1981, *Astron. Astrophys.* **94**, 100.
Benz, A. O., Zlobec, P., and Jaeggi, M.: 1982, *Astron. Astrophys.* **109**, 305.
de Groot, T.: 1962, *Inf. Bull. Solar Radio Obs. Europe* **9**, 4.
Dennis, B. R., Benz, A. O., Ranieri, M., and Simnett, G. M.: 1984, *Solar Phys.* **90**, 383.
Dröge, F. and Riemann, P.: 1961, *Inf. Bull. Solar Radio Obs. Europe* **8**, 6.
Elgarøy, O.: 1962, *Inf. Bull. Solar Radio Obs. Europe* **9**, 3.
de Jager, C. and de Jonge, G.: 1978, *Solar Phys.* **58**, 127.

Kane, S. R.: 1981, *Astrophys. J.* **247**, 1113.
Kane, S. R. and Benz, A. O.: 1985, in preparation.
Kuijpers, J., van der Post, P., and Slottje, C.: 1981, *Astron. Astrophys.* **103**, 331.
Malville, J. M., Aller, H. D., and Jensen, C. J.: 1967, *J. Astrophys.* **147**, 711.
Melrose, D. B. and Dulk, G. A.: 1982, *Astrophys. J.* **259**, 844.
Perrenoud, M. R.: 1982, *Solar Phys.* **81**, 197.
Sharma, R. R., Vlahos, L., and Papadopoulos, K.: 1982, *Astron. Astrophys.* **112**, 377.
Slottje, C.: 1978, *Nature* **275**, 510.
Slottje, C.: 1980, in M. R. Kundu and T. E. Gergeley (eds.), 'Radio Physics of the Sun', *IAU Symp.* **86**, 195.
Strong, K. T., Benz, A. O., Dennis, B. R., Leibacher, J. W., Mewe, R., Poland, A. I., Schrijver, J., Simnett, G. M., Smith, J. B., ad Sylvester, J.: 1984, *Solar Phys.* **91**, 325.
Tarnstrom, G. L. and Pilipp, K. W.: 1972a, *Astron. Astrophys.* **16**, 21.
Tarnstrom, G. L. and Pilipp, K. W.: 1972b, *Astron. Astrophys.* **17**, 267.
Vlahos, L., Sharma, R. R., and Papadopoulos, K.: 1983, *J. Astrophys* **275**, 376.
Wiehl, H. J., Benz, A. O., and Aschwanden, M. J.: 1984, *Solar Phys.*, in press.
Zhao, R. and Yin, S.: 1982, *Scientia Sinica* **25**, 422.
Zheleznyakov, V. V. and Zaitsev, K. V.: 1975, *Astron. Astrophys.* **39**, 107.